

Performance assessment of specialist conductive paint for cathodic protection of steel in reinforced concrete structures

Goyal, A., Sadeghi Pouya, H. & Ganjian, E.

Author post-print (accepted) deposited by Coventry University's Repository

Original citation & hyperlink:

Goyal, A, Sadeghi Pouya, H & Ganjian, E 2019, 'Performance assessment of specialist conductive paint for cathodic protection of steel in reinforced concrete structures' *Construction and Building Materials*, vol. 223, pp. 1083-1094.
<https://dx.doi.org/10.1016/j.conbuildmat.2019.07.344>

DOI 10.1016/j.conbuildmat.2019.07.344

ISSN 0950-0618

ESSN 1879-0526

Publisher: Elsevier

NOTICE: this is the author's version of a work that was accepted for publication in *Construction and Building Materials*. Changes resulting from the publishing process, such as peer review, editing, corrections, structural formatting, and other quality control mechanisms may not be reflected in this document. Changes may have been made to this work since it was submitted for publication. A definitive version was subsequently published in *Construction and Building Materials*, 223, (2019) DOI: 10.1016/j.conbuildmat.2019.07.344

© 2019, Elsevier. Licensed under the Creative Commons Attribution-NonCommercial-NoDerivatives 4.0 International

<http://creativecommons.org/licenses/by-nc-nd/4.0/>

Copyright © and Moral Rights are retained by the author(s) and/ or other copyright owners. A copy can be downloaded for personal non-commercial research or study, without prior permission or charge. This item cannot be reproduced or quoted extensively from without first obtaining permission in writing from the copyright holder(s). The content must not be changed in any way or sold commercially in any format or medium without the formal permission of the copyright holders.

This document is the author's post-print version, incorporating any revisions agreed during the peer-review process. Some differences between the published version and this version may remain and you are advised to consult the published version if you wish to cite from it.

1 Performance Assessment of Specialist Conductive Paint for Cathodic Protection of Steel in 2 Reinforced Concrete Structures

3 Arpit Goyal¹

4 PhD scholar, Centre of Build and Natural Environment, Sir John Laing Building, Coventry University, Coventry, CV1 2HF, United Kingdom, Email:
5 goyala4@uni.coventry.ac.uk

6 Homayoon Sadeghi Pouya

7 Research Fellow, Centre for the Build and Natural Environment, Engineering, Environment, & Computing Building, Coventry University, Coventry,
8 CV1 2JH, United Kingdom, Email: H.Sadeghipouya@coventry.ac.uk

9 Senior Materials Engineer, Structural Rehabilitation, Transportation UK and Europe, Atkins, Birmingham, United Kingdom,
10 Homayoon.Sadeghipouya@atkinsglobal.com

11 Eshmaiel Ganjian

12 Professor, Centre for the Build and Natural Environment, Engineering, Environment, & Computing Building, Coventry University, Coventry, CV1
13 2JH, United Kingdom, Email: e.ganjian@coventry.ac.uk

14

15 Abstract

16 ICCP system provides effective corrosion protection in a chloride environment. This research
17 evaluates the feasibility of zinc rich paints (ZRP) as ICCP anode for RC structures. The preliminary
18 investigation showed the application of three layers of ZRP with medium concrete surface roughness
19 and use of Cu/Nb/Pt wire as primary anode gives maximum bond strength and uniform current
20 distribution across the ZRP coating. Moreover, polarization results showed satisfactory performance
21 of the ZRP anode coating subjected to a current density of 12.5 mA/m². Anode was found to be
22 vapour permeable and effectively provide protection with a service life up to 15 years.

23 **Keywords:** Steel reinforced concrete; Conductive Paint; Microstructure, Coating Anode; Cathodic
24 Protection; Service Life, Permeability, Polarization

25 1.0 Introduction

26 One of the major challenges of recent years in the construction industry has been to extend the service
27 life of reinforced concrete structures, especially those exposed to the coastal environment [1]. The

¹ Corresponding author

28 corrosion of steel reinforcement in concrete structures leads to rust formation, cracking, delamination
29 and degradation of structure and is considered as the biggest factor for the damage in bridges and
30 construction industries [2–4]. To deal with the issue many researchers have studied and developed
31 various corrosion mitigation techniques which include conventional patch repair, corrosion inhibitors
32 and electrochemical treatment. Electrochemical techniques such as cathodic protection, cathodic
33 prevention, electrochemical realkalisation and electrochemical chloride extraction are proved as
34 effective methods for corrosion prevention and mitigation [5–7]. Impressed Current Cathodic
35 protection (ICCP) has proven to be the most effective approach for preventing and minimizing
36 corrosion initiation in RC structures subjected to high chloride environment [8–12]. The principle of
37 ICCP is to negatively shift the steel/concrete/electrode potential of the protected structure by
38 delivering sufficient polarization current, such that initiation and propagation of corrosion are
39 suppressed and corrosion failure will not occur during the lifetime of the structure, pitting is prevented
40 and steel becomes passivated [9,13–15].

41 The most critical component of any cathodic protection is the design of an effective anode system to
42 distribute protection current efficiently and economically to the structural elements to be protected.
43 Also, it must be easy to install and possess long term durability. For ICCP of reinforced concrete,
44 research has been centred on the development of anode materials, e.g. thermal sprayed zinc [16–24],
45 titanium anodes [25,26], conductive coating [27–31], and conductive cementitious overlay anodes
46 [9,32–35]. However, the researchers are still trying to find new anode materials with improved
47 performance characteristics, such as higher bond strength, lower acidification, low cost and improved
48 installation convenience [11].

49 Conductive coating anode systems include organic and mineral coating containing a variety of
50 formulations of carbon pigmented solvent or water dispersed coatings and metallic coatings such as
51 thermal sprayed zinc. Zinc based anodes are mostly preferred for their application in reinforced
52 concrete [8,36]. However, its use is limited mainly as sacrificial anodes [37]. Generally, they are used

53 as part of patch repair system to enhance the longevity of the repairs with an estimated life time of
54 around 10 years. Sergi and Whitmore [22] reported the performance of sacrificial zinc anodes in
55 concrete after monitoring them for 10 years and they were successful in providing the required
56 current. Sekar *et al.* [29] used zinc overlay as a sacrificial anode and observed that potential shift is
57 considerable near the anode and decreases on increasing distance from the anode, implying non-
58 uniform current distribution. Thus, the use of zinc as sacrificial anode cathodic protection (SACP)
59 does not show a uniform distribution of current [29]. Moreover, it has been observed by many
60 researchers that galvanic zinc is unable to deliver the required current unless it is periodically wetted
61 [19,33,38,39]. However, its current delivery could be restored by either direct wetting the anode [38]
62 or by using humectants [27,37,40–42]. Humectant solutions keep up the moisture level in the concrete
63 thus reducing the electrical resistivity of concrete and anode concrete interface [40,42]. Hence,
64 galvanic zinc anode systems without humectants should only be applied in the aggressive
65 environment such as high humidity, soils or wet/dry condition, because only in these conditions they
66 are able to fulfil required current demand to satisfy the 100 mV decay performance criterion [43].

67 Various forms of zinc (Zn) anodes have been developed such as thermally or arc sprayed coating of
68 Zn, Zn-Al or Al-Zn-In and rolled zinc sheets. Thermally sprayed zinc (TSZ) anodes are found to be
69 more effective to be used as an ICCP anode, however, can be used for both sacrificial and ICCP
70 systems [34,37]. The main failure reason for thermal sprayed zinc as ICCP systems is the loss of bond
71 between anode and concrete substrate or high voltage demand greater than operating limits [44].
72 During operation with SACP with TSZ anode, Dugarte and Sagues [45] observed oxidation products
73 of Zn (white corrosion product) at Zn-cement interface leading to loss of bond [45]. For long term
74 performance of TSZ anode, it is essential to maintain moisture at Zn-concrete interface. This lowers
75 the voltage needed for the effective operation of ICCP systems, increases the performance of the
76 sacrificial system, and redistribute anode dissolution products into the concrete pore structure [16].
77 Rolled Zinc Sheet and metallized Zn-Al is found unsuitable for ICCP as they lead to blistering and
78 loss of adhesion [34,46]. The driving voltage i.e. potential between zinc sheet and steel was observed

79 to be very high for an impressed current mode which is unsuitable for CP of reinforced concrete
80 resulting in debonding [46].

81 On the other hand, Zinc-rich paints (ZRPs) are efficiently used as an anti-corrosion paint on ferrous
82 metals and as a substitute to hot-dip galvanizing [47,48]. They can be easily applied by roller, brush
83 or spray and thus can be advantageous over other anodes.

84 Zinc anodes for protecting RC structures can be found in numerous references. However, the
85 literature search indicated limited work on Zinc Rich Paint (ZRP) as a CP anode for concrete
86 structures. This paper provides the first systematic electrochemical examination of ZRP as an anode
87 system for the ICCP. This paper is a result of joint collaboration with Atkins Transportation to
88 develop the basis of design and document electrochemical properties of ZRP for use in cathodic
89 protection of chloride contaminated reinforced concrete structures. The primary objective of this
90 study was to evaluate the feasibility of using ZRP as an anode for the ICCP system.

91 **2.0 Experimental Investigation**

92 **2.1 Materials**

93 For this research, a commercially available solvent based zinc-rich paints containing zinc powder,
94 aromatic hydrocarbons, and a binder has been used. This paint can be applied by brush, roller,
95 spraying, or dipping under any atmospheric condition. For now, it is not possible for authors to
96 disclose further information regarding the paint material due to commercial confidentiality.

97 **2.2 Specimen Preparation**

98 All the concrete specimens of C32/40 grade were cast during the study with water cement ratio of 0.5
99 which is a similar grade for existing aged structures. The mix proportioning is finalized after
100 successful trial mixing as per BS 1881-125:2013 [49]. The details of mix proportions of specimens
101 are shown in **Table 1**. 3% NaCl solution by weight of cement was deliberately added to the mixing
102 water during casting as specified in the NACE Standard TM0294-2007 [50]. Specimen size varied

103 with the type of experiment and described in the respective sections. Specimens were demoulded
 104 after 24 hours and cured in salt solution at $20\pm 1^{\circ}\text{C}$ for a total period of 28 days. Three specimens
 105 were tested for each test.

106 **Table 1-** Mix proportioning of concrete specimens

Mix	w/c Ratio	Water	Cement	Sand	Gravel	Chloride
					(max 20mm)	
				kg/m ³		kg/m ³
3% chloride	0.5	180	360	640.5	1189.5	10.8

107

108 2.3 Coating Application

109 Various application and surface preparation methods have been explored [51], without deviating
 110 significantly from the best practice for the application of the coating on construction site and the best
 111 one is chosen here as a preferred method of application. Concrete surface was prepared by wire
 112 brushing the concrete surface for 15-20 min exposing a finer proportion of aggregates and removing
 113 the laitance layer. After surface preparation, specimen surface was cleaned for any dust using non-
 114 contaminated compressed air before coating. Then, the paint was thoroughly mixed using a high shear
 115 mixer to achieve a homogeneous liquid and then applied on the specimen surface, by a paint roller in
 116 3 layers. The total thickness of paint was maintained in the range of 200-350 μm . Each layer of the
 117 paint was allowed to atmospherically dry for a total period of 24 hours before application of the next
 118 layer.

119 3.0 Experimental Tests and Procedure

120 3.1 Bond Strength

121 The bond strength test was carried out using Elcometer 106/6 Adhesion equipment as shown in **Fig.**
 122 **1**. Concrete cubes of size 100 \times 100 \times 100 mm were cast for the test. The substrate was cured in potable
 123 water for 28 days then, allowed to air dry for at least a month prior to coating and pull-off tested as
 124 recommended by ASTM D7234 – 12 [52]. After the completion of the coating, a metallic disc of 20
 125 mm diameter was attached to the specimens by using epoxy. The bond strength test was performed
 126 after full curing of the epoxy resin i.e. after 24 hours. The bond strength was evaluated using the pull

127 out test method, in which the anode overlay was pulled to determine its bond with the substrate. The
128 pull off force was manually applied on the disc until the failure of the bond was achieved.



129 **Fig. 1-** Bond strength test setup

130 **3.2 Permeability property of coating**

131 Permeability property of coating was measured in terms of water absorption and water vapour
132 transmission as per BS 1062-3 [53] and BS EN ISO 7783:2018[54] respectively. For water
133 absorption, concrete specimens of 100 mm diameter and 50 mm thickness were cured for 28 days,
134 coated on one side only and then initial conditioned at $50\pm 2^{\circ}\text{C}$ temperature and $80\pm 3\%$ RH for 3 days.
135 The specimens were then placed in water with the coated surface facing the water side and weight
136 gain was measured for 7 days after placing the specimen in water. The water absorption rate was then
137 computed as per the standard [50].

138 ZRP been a non-self-supporting coating, was applied on the porous substrate and tested for water
139 vapour transmission using cup method. The cup is filled with water and the amount of moisture loss
140 through the coating covering the mouth of the cup is measured by subsequent weighing as per the
141 standard [51].

142 **3.3 Polarization Test**

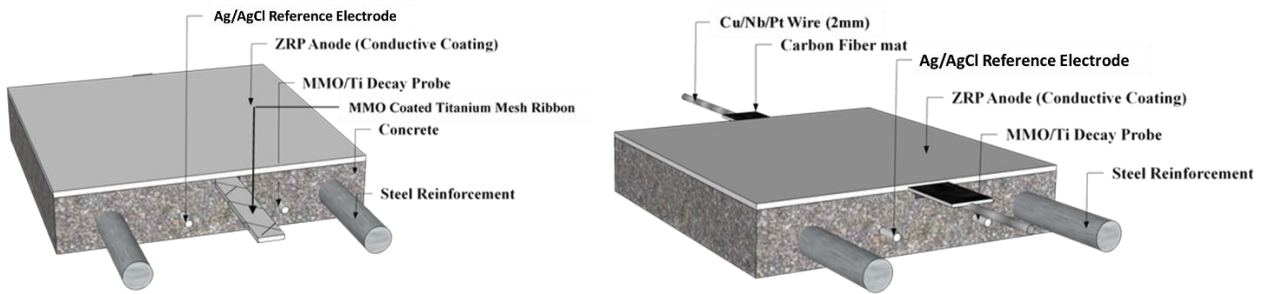
143 The principle of this test is to assess the performance of ZRP coating anode for ICCP system installed
144 to reinforced concrete elements and evaluate the following characteristics:

- 145 (i) Identify the primary conductor best suited for uniform current distribution across ZRP anode
146 coating.

147 (ii) Cathodic Polarization of the steel reinforcement in concrete by the ZRP anode.

148 This test was carried out on three similar slab specimens of size 200×200×70 mm. Two ribbed steel
149 bar of 10 mm diameter with allowance for 50 mm cover were embedded in the slab. The exposed
150 length of the steel bar in contact with concrete inside the specimen was 100 mm. The exposed end of
151 each rebar outside the mould has been covered with a heat-shrink sleeve to protect it from corrosion
152 when the specimen is placed in water and /or salt solution. Each specimen contains one miniaturized
153 mixed metal oxide/titanium (MMO/Ti) and one Ag/AgCl/0.5M KCl reference electrode to monitor
154 steel/concrete/electrode potential.

155 For the first part of the experiment, two types of primary anode conductors were used (i) MMO
156 Coated Titanium Mesh Ribbon and (ii) Anomet platinum clad wire. Anomet platinum clad wire is
157 covered with a carbon fibre mat to protect it from any physical damage. The schematics of the
158 connections are shown in **Fig. 2**. **Table 2** gives the total dry coat thickness (DFT) of paint on each
159 specimen.



160 **Fig. 2-** Schematic of polarization test specimens with (a) MMO/Ti ribbon primary anode (b)
161 Anomet platinum clad wire primary anode

162 **Table 2-** Dry film thickness of ZRP Coating on slab specimens

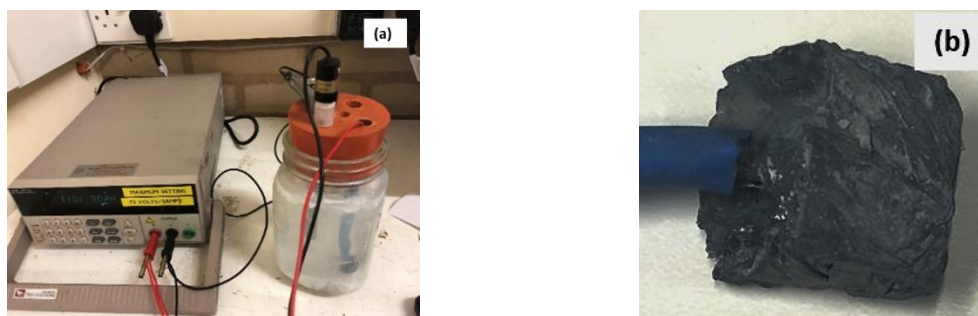
Slab	Dry Coat			Total Thickness (µm)
	First Coat Thickness (µm)	Second Coat Thickness (µm)	Third Coat Thickness (µm)	
Slab 1	110	99	73	282
Slab 2	97	92	86	275
Slab 3	99	94	88	281

163 The effectiveness of the primary anode conductor was assessed by potential mapping versus an
164 external reference electrode (Ag/AgCl/0.5M KCl) before and during polarization. This is done to

165 identify the most efficient primary anode conductor that can distribute current within the coating with
166 minimum loss of voltage. The specimens were polarized at six levels of current density, i.e., 10, 20,
167 30, 40, 50 and 60 mA/m² of steel surface area, which were approximately 3.125, 6.25, 9.375, 12.5,
168 15.625 and 18.75 mA/m² of the anode surface area. The polarization and depolarization behavior of
169 steel in concrete specimens were recorded every minute using a data logger. The polarization recorded
170 were 'ON' potentials when the system was energised. For both polarization and depolarization tests,
171 specimens were partially immersed in the 3% salt solution up to the rebar level in temperature and
172 humidity controlled room since starting of the experiment. Hence, the moisture content of the samples
173 remains constant throughout but not fully saturated. For initiating cathodic protection current in the
174 specimen, negative terminal of the power supply was connected to the steel bars and the positive
175 terminal to the primary anode conductor. Specimens were polarized for 5 days and then 24 hours
176 depolarization was recorded. Each specimen was tested for each current density with decay period in
177 between at the same time using separate power supplies to keep the environmental conditions same.
178 The final depolarization was then analyzed to determine whether protection criterion was met in
179 accordance with BS EN ISO 12696:2016 [37].

180 3.4 Service life test

181 The principle of this test is to get an indication of anodes ability to perform satisfactorily for a specific
182 number of years. The test was performed in accordance with NACE TM0294 [50]. The accelerated
183 test requires passing high current to concrete, which may lead to its premature failure, thus test was
184 performed in an aqueous solution. The setup required is shown in **Fig. 3(a)**.



185 **Fig. 3** (a) Setup for service life test (b) ZRP Block

186 A 20×20×20 mm ZRP block with Anomet platinum clad wire at the centre of the block for electrical
187 connection was cast by filling the mould with paint and then oven dried at 40°C, as seen in **Fig. 3(b)**
188 and used as an anode. The anode area was approximately 20 cm² after drying. For the cathode, 12.7
189 mm diameter titanium rod was used. Test cell used was a beaker fitted with a rubber stopper at the
190 top to hold the electrodes and reduce air contact. Saturated calomel electrode was used as a reference
191 electrode and a 3% NaCl solution was used as an electrolyte. Two additional holes were located on
192 the stopper, one to vent gases away from the electrical connection and other to measure the pH of the
193 test solution.

194 The anode was polarized at a constant current of 17.8 mA as per standard. Parameters such as cell
195 voltage, cell current, anode potential vs SCE reference electrode and pH of the electrolyte were
196 recorded every minute in the data logger until anode failure which is marked by a rapid escalation in
197 both cell voltage and anode potential. The time of failure is recorded when the anode potential
198 increased by 4.0 V above its initial value.

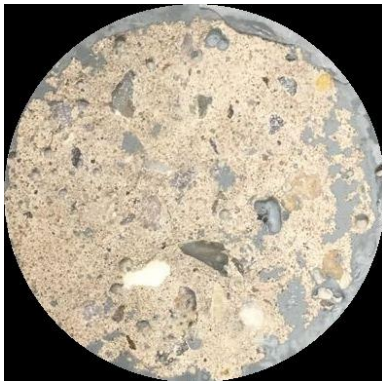
199 **3.5 Characterization of coating and coating-concrete interface**

200 The oxidation products formed on the ZRP block after service life was analyzed using X-ray
201 diffraction (XRD). All the experiments were carried out at room temperature using copper radiation
202 (Cu-K α). The values of test parameters such as scan speed and range of 2 θ were 0.03°/sec and 10° to
203 90°, respectively. Also, Field Emission Scanning Electron Microscopy (FE-SEM) analysis was
204 performed to study the microstructure of the coated sample and to study the zinc oxidation products
205 formed during polarization at an accelerating voltage of 15-20kV. Samples were taken from
206 polarization specimens after the test, grounded and cold mounted. The microstructures of the prepared
207 samples were examined using secondary electron (SE) in a Zeiss Gemini Sigma 500VP scanning
208 electron microscope (SEM) and EDS.

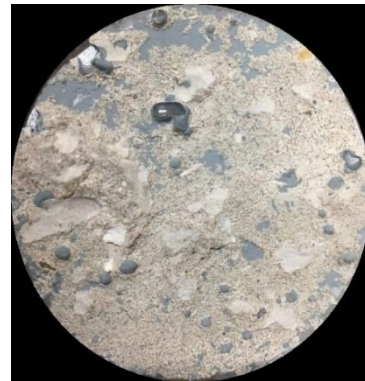
209 **4.0 Experimental Results and Discussion**

210 **4.1 Bond Strength**

211 For the bond strength test, both failure load and failure mode were recorded. The average pull off
212 failure stress obtained was 2.73 MPa. This may be due to the minimal or null amount of aggregates
213 exposed in the immediate dolly testing position in substrate preparation. The amount of aggregates
214 exposed has a direct influence upon the pull-off strength since the bond interface between the coating
215 and the exposed aggregate(s) is weakened due to the inherent smooth surface of the aggregate [55].
216 The observed pull of strength for MR substrate roughness is greater than the required value of 1.5
217 MPa (for flexible systems with trafficking) and 2.0 MPa (for rigid systems with trafficking)
218 recommended by BS EN 1504-2:2004 [56]. Thus, the ZRP paint used satisfies the bond strength
219 requirement.



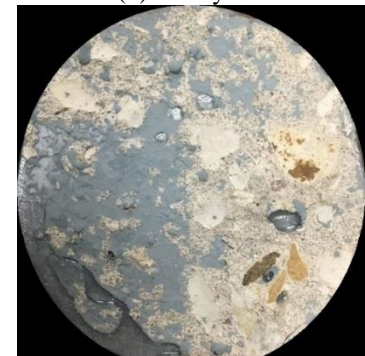
(a) Substrate end- S1



(b) Dolly end- S1



(c) Substrate end- S2



(d) Dolly end- S2



(e) Substrate end- S3



(f) Dolly end- S3

Fig. 4- Bond strength test failure mode of different surface roughness

220

221 **Fig. 4** illustrates failure modes for prepared surface profile and the detailed failure mechanism is
 222 given in **Table 3**. Mode of failure is an important factor when the specimens are tested for bond
 223 strength as it gives a clear indication of the bond that occurred between the two layers. As observed
 224 in **Fig. 4**, the main failure was within the substrate giving higher bond strength.

225

Table 3- Bond strength and failure mode for different samples

Specimen No.	T _{env.} (°C)	RH _{env.} _{nv} (%)	T _{substrate} (°C)	DFT (μm)	σ (MPa)	σ _{av} (MPa)	Failure Type	Area of Fracture (%)
1	20.0	60.0	24.0±0.25	319	2.90		A, B/C	A = 98, B/C = 2
2	±1.0	±2.0	24.0±0.25	314	2.70	2.73	A, B/C	A = 95, B/C = 5
3			24.5±0.25	319	2.60		A, B/C	A = 92, B/C = 8

* T_{env.} (°C) = environmental temperature, RH_{env.} (%) = environmental relative humidity, T_{substrate} (°C) = substrate temperature, DFT (μm) = dry film thickness, σ_{av} (MPa) = average pull-off stress, A = failure occurring within concrete substrate, A/B = failure between concrete substrate and coating, B/C = inter-coat failure, -/Y = failure between adhesive and coating

226 Changes in the bond strength after the polarization current is applied and any deleterious effect of
 227 acidification is outside the scope of this study.

228 4.2 Permeability property of coating

229 **Table 4** shows the water absorption rate of the ZRP coating. It can be seen that the coating reduces
 230 the absorption of water by concrete. The water transmissibility of coating was found to be 0.0018
 231 kg/m².h^{0.5}, which was 14% lower as compared to concrete without coating. The water transmissibility
 232 of coating found was less than 0.1 kg/m².h^{0.5}, hence as per BS EN 1504-2:2004 [56], coating restricts
 233 diffusion of chloride ions and capillary water absorption.

234

235

Table 4- Water absorption rate for ZRP coated and uncoated sample

Sample	Water Absorption Rate (kg/m ² /h)	Water Vapour Transmission (WVT)	
		WVT Rate g/m ² /h	Equivalent air layer thickness, s _D (m)
Uncoated sample	2.1×10 ⁻³	-	-
Coated sample	1.8×10 ⁻³	1.3	0.65

236

237

238

239

240

Performance of coating is also affected by its capability of aiding or restricting the passage of water vapour. For ZRP coating, water vapour transmission rate was found to be 1.3g/m²/hr with an equivalent layer thickness (s_D) of 0.65m. Hence coating comes under class 1 (s_D < 5m) coating and is permeable to water vapour as per BS EN 1504-2:2004 [56]. Thus, the ZRP coating allows moisture to evaporate and prevents long term debondment and premature failure.

241

4.3 Primary Anode Selection

242

243

244

245

246

247

248

249

For reinforced concrete, the primary anode is required for most ICCP system [57]. The main purpose of the primary anode conductor is to distribute the current along the conductive coating (secondary anode). The most common primary anodes used for cathodic protection in reinforced concrete are Platinized titanium or niobium wires, Platinized mixed-metal-oxide (MMO)-coated titanium and Titanium wires or strips [57]. In this study, two types of primary anodes were used i.e. MMO coated titanium mesh ribbon and Anomet platinum clad wire. Half-cell potential drop along the secondary anode was measured by using Ag/AgCl/0.5M KCl reference electrode placed on the surface of the ZRP coating.

250

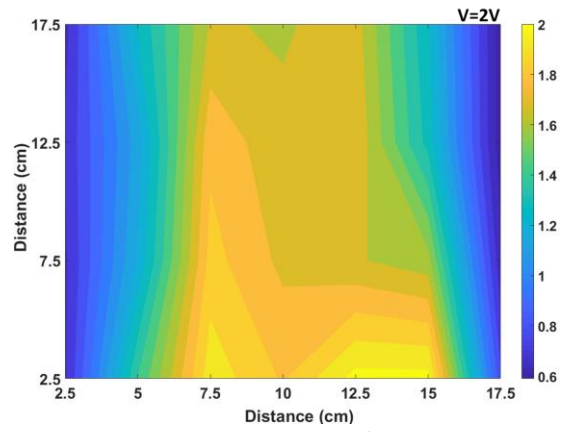
251

252

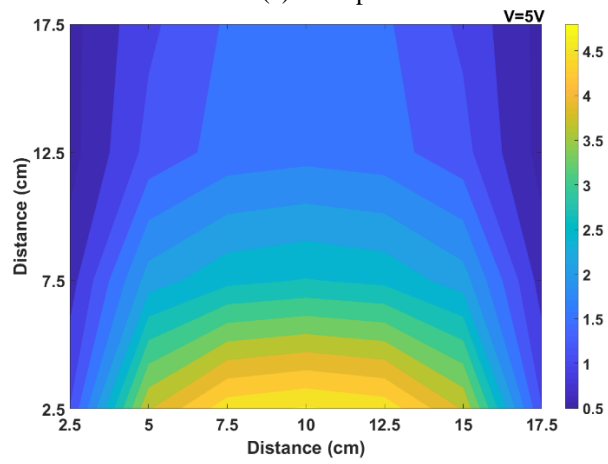
253

254

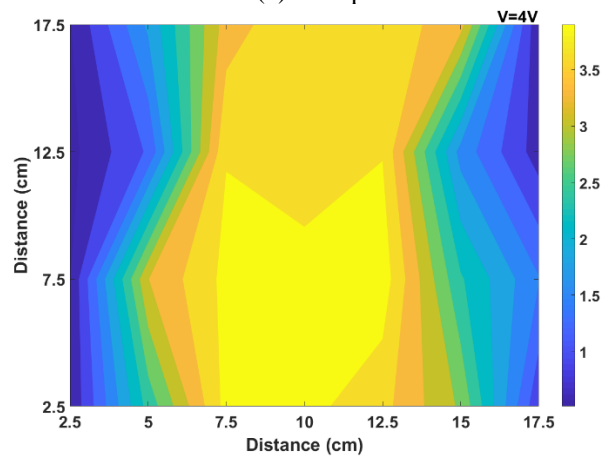
Fig. 5 and **Fig. 6** presents the contour plot for wire and ribbon primary anode conductor respectively, showing the current distribution across the ZRP coating during polarization. The applied current density during polarization was 40mA/m². Steel/Concrete/Electrode Potential was measured at 2.5, 5 and 7.5 cm from the primary anode on both sides. For all the specimens, more uniform current distribution is obtained by using Anomet platinum clad wire compared to ribbon anode.



(a) Sample 1

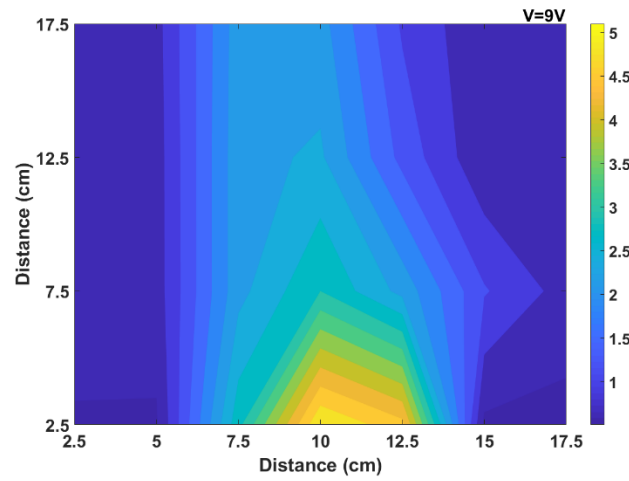


(b) Sample 2

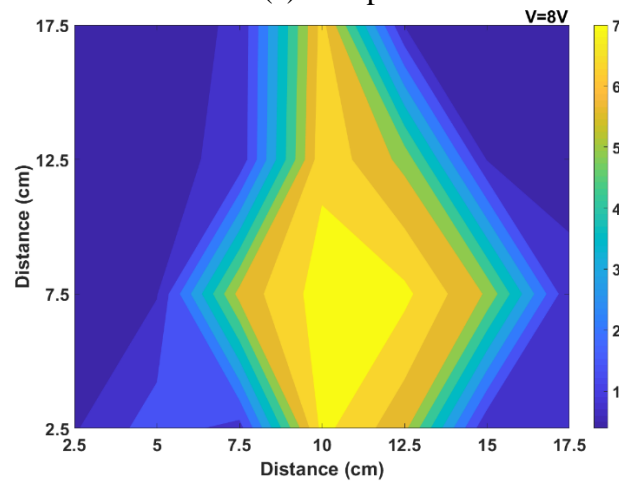


(c) Sample 3

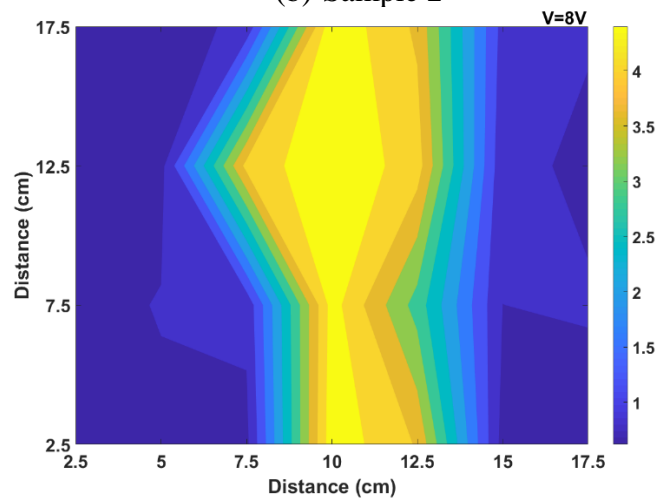
255 **Fig. 5-** Contour plots of Steel/Concrete/Electrode potential (V) across the coating before and during
 256 polarization with Anomet wire primary anode



(a) Sample 1



(b) Sample 2

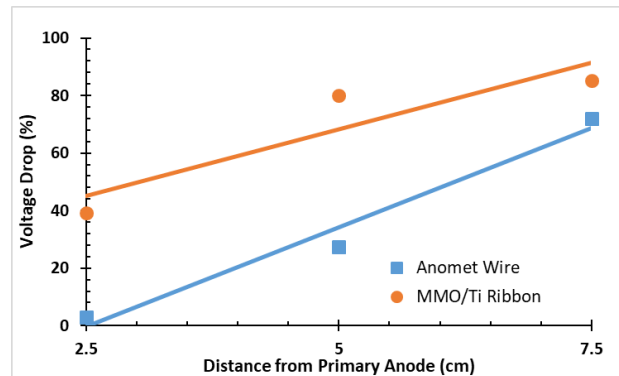


(c) Sample 3

257 **Fig. 6-** Contour plots of Steel/Concrete/Electrode potential (V) across the coating before and during
 258 polarization with MMO/Ti ribbon primary anode

259 **Fig. 7** shows percentage of the potential drop across the ZRP paint as a function of distance from the
 260 primary anode. It can be observed that in case of primary wire anode there was only 3% potential
 261 drop at 2.5cm from primary anode conductor which increased to 27.3% and 71.9% at 5cm and 7.5cm

262 respectively on both sides of the primary anode. Whereas in case of primary ribbon anode, at a
263 distance of 2.5cm from the primary anode the potential dropped by almost 40%, which further
264 reduced by 80.1% and 85.6% at 5cm and 7.5cm respectively. Moreover, the as-found voltage (V)
265 required to achieve the current density of 40 mA/m² to polarize the slabs sufficiently was only 3.0 V
266 in case of primary wire anode. MMO/Ti ribbon primary anode requires almost three times the as-
267 found voltage as compared to primary wire anode.



268

269 **Fig. 7-** Potential drop across the ZRP paint as a function of distance from primary anode

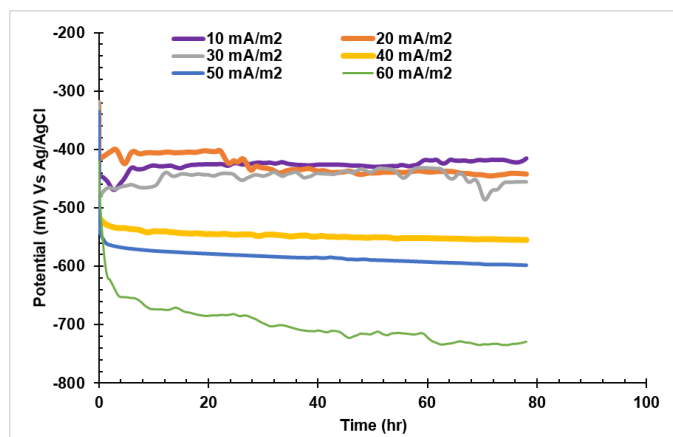
270

270 Hence, it can be observed that a reasonable current distribution could be obtained by using Anomet
271 platinum clad wire as a primary anode conductor since it showed a more uniform current distribution
272 with the least potential drop across the ZRP coating anode. For MMO/Ti ribbon anode, uniform
273 coating is difficult, whereas, Anomet wire anode gives more uniform coating and better current
274 distribution. Moreover, risk of pitting is not an issue for Anomet wire, the as-found voltage can go
275 up to 12V. Thus, for monitoring of the efficiency and electrochemical properties of ZRP anode paint
276 as a secondary anode for cathodic protection of steel in concrete, cathodic polarization test was carried
277 out using Anomet platinum clad wire as a primary anode.

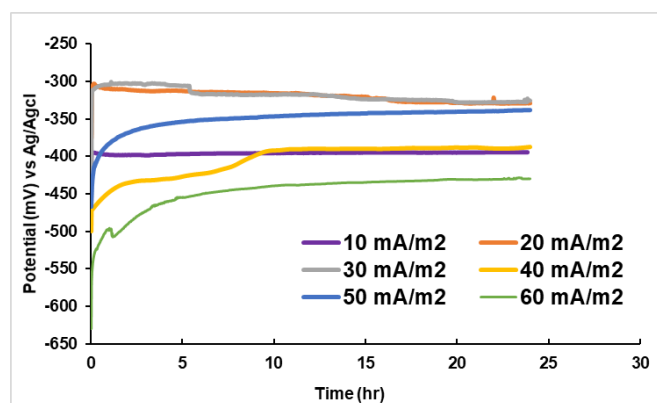
278 4.4 Polarization Test

279 This phase of testing involves the determination of required current density to meet the cathodic
280 protection performance criteria as per BS EN 12696 i.e. a) 'Instantaneous OFF' potential more
281 negative than -720 mV (vs Ag/AgCl/0.5M KCl) or b) 100 mV decay criterion over a maximum of 24

282 hours. The current density, ‘Instant-OFF’ potential, 4-hour decay and 24-hour polarization decay
 283 criteria were used to evaluate the ZRP as an anode system for ICCP system.



284 **Fig.8-** Electrochemical performance of specimens at various current densities with respect to
 285 Ag/AgCl/0.5M KCl electrode



286 **Fig. 9-** Depolarization behaviour of specimens at various current densities with respect to
 287 Ag/AgCl/0.5M KCl electrode

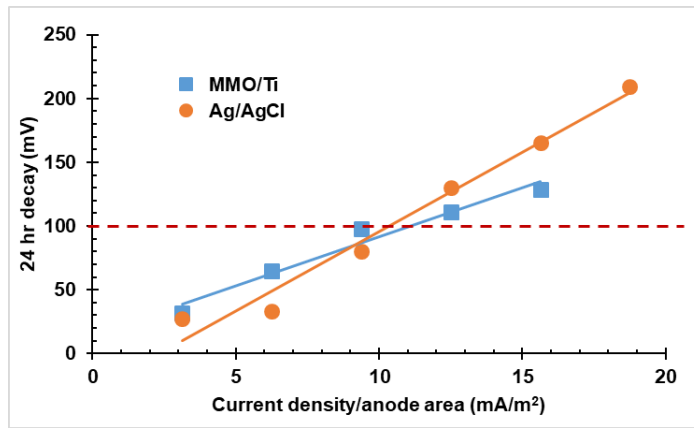
288 **Fig. 8** and **Fig. 9** shows the polarization and depolarization behaviour evaluation of the ZRP anode
 289 with six different current densities (10, 20, 30, 40, 50 and 60 mA/m² per steel surface area) [3.125,
 290 6.25, 9.375, 12.5, 15.625 and 18.75 mA/m² per anode surface area] respectively. Results are
 291 summarized in **Table 5**.

292 **Table 5-** Summary of polarization test results

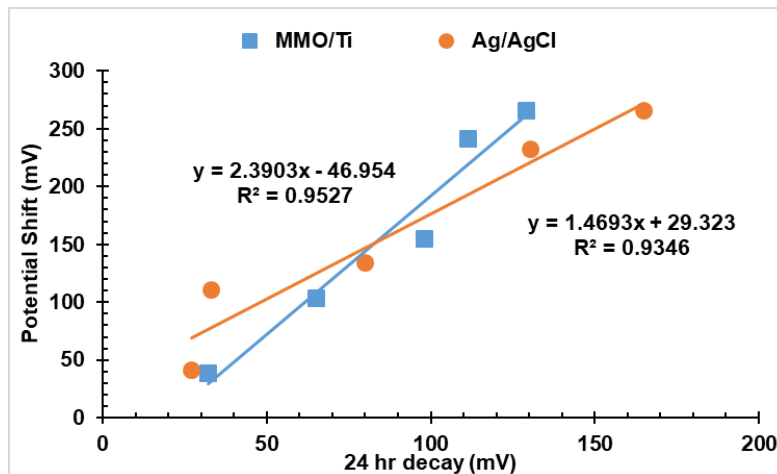
Current density/ steel area mA/m ²	Current density/ anode area mA/m ²	Pre energization Potential (mV)	'Instant off' potential (mV) Vs		4 hr decay (mV) Vs		24 hr decay (mV) Vs		Voltage across anode (V)
			MMO/Ti	Ag/AgCl/0.5MKCl	MMO/Ti	Ag/AgCl/0.5MKCl	MMO/Ti	Ag/AgCl/0.5MKCl	
10	3.13	-323	-462	-411	28	13	32	16	1.5-2.5
20	6.25	-320	-414	-376	60	41	67	48	2-3
30	9.38	-318	-432	-383	83	57	98	80	2.5-4
40	12.50	-300	-546	-486	94	108	130	181	3-4
50	15.63	-342	-525	-498	143	110	164	153	4-5
60	18.75	-338	-641	-630	175	168	209	200	5-7

293 The findings from the evaluation are summarized as follows:

- 294 • There is a significant potential rise in first 5 hours of polarization, after which potential is still
295 rising but at a slower rate. Potential rise increases with an increase in polarization current density.
296 The difference between ‘ON’ potential and instantaneous ‘OFF’ potential was in the range of 10-
297 70 mV (vs Ag/AgCl/0.5M KCl).
- 298 • The average 4-hour and 24-hour decay increases as polarization current density increases.
299 However, all the specimens met the 100 mV decay polarization criterion only when polarized
300 with 40, 50 and 60 mA/m² of current density per steel surface area [12.5 and 15.625 mA/m² per
301 anode surface area]. Also, even after depolarization, passivation was still not reached as observed
302 from the results, thus not affecting the interpretation of the next current density. Anodes were
303 tested for higher current density to see its ability to achieve and sustain the design current densities
304 recommended in BS EN ISO 12696 at 1:1 steel: anode surface area ratio.
- 305 • **Table 5** shows voltage across the coating when a constant current is supplied through the power
306 supply. It can be seen that for all current densities used, the as-found voltage (V) across the anode
307 was below 10V. The as-found voltage increases with an increase in supplied current density and
308 showed a similar trend as decay values. At a current density of 40 mA/m², the average as-found
309 voltage across the anode was 3 V.
- 310 • **Fig. 10** shows that the optimized current density required for successful application of ZRP as an
311 anode for ICCP is 40mA/m² of steel surface area, equivalent to 12.5 mA/m² of anode surface area,
312 meeting BS EN 12696 [37] criterion (b). 40mA/m² is equivalent to 17.2kC/m² of charge passed,
313 which is quite less than 50kC/m² required to stop corrosion [6]. However, it still satisfies the 100
314 mV decay criterion which is the main aim of the test. For atmospherically exposed concrete
315 polarized for a longer period of time, this could be met with lower current density due to reduced
316 corrosion rate as a result of higher concrete resistivity and lower moisture content in dry
317 conditions.



318 **Fig. 10-** Correlation between potential decay over 24 hours and polarization current density
 319 • **Fig. 11** shows the correlation between 24 hour decay and Steel/Concrete potential shift w.r.t.
 320 MMO/Ti ($R^2 = 0.96$) and Ag/AgCl/0.5M KCl reference electrode ($R^2 = 0.94$) and showed a
 321 quadratic relationship between the two. Higher the potential shift, higher is the decay. From the
 322 graph, it can be calculated that for 100 mv 24 hour decay and considering the tested specimen age
 323 and conditions, at least 98.8 mV (vs Ag/AgCl/0.5M KCl) of potential shift over a period of 4 days
 324 is required. In practice, long term polarization may be needed.



325 **Fig. 11-** Correlation between potential decay over 24 hours and Steel/Concrete potential shift

326 **4.5 Service Life Test**

327 Anode was polarized at a constant current of 17.8 mA until anode failure, which is marked by an
 328 increase of anode potential by 4.0 V above its initial value. Results are shown in **Table 6**. Total time
 329 of polarization before failure was 12 days. Moreover, the pH of the test solution changed from 8.5 to
 330 11.8 during the polarization period, indicating formation of some oxides or hydroxides.

Table 6- Results of Anode Life Testing in 30 g/L NaCl Solution

Test	Time	Cell current (mA)	Cell voltage (V)	Anode potential vs SCE (V)	pH
Reverse Current	1 min	-17.00	1.28		
	1 h	-17.28	1.23		
	8.8 h	-17.91	1.11		
Normal Current	1 h	-17.81	-0.70	0.91	8.5
	1 day	-17.85	-0.79	0.78	-
	2 days	-17.80	-1.01	0.37	-
	3 days	-17.91	-1.60	-0.21	-
	4 days	-17.50	-2.21	-0.82	-
	5 days	-16.60	-2.88	-1.55	-
	6 days	-17.30	-4.39	-2.98	-
	7 days	-17.18	-4.34	-2.99	-
	8 days	-17.18	-4.31	-2.97	-
	9 days	-17.34	-4.33	-2.98	-
	10 days	-18.56	-4.40	-3.07	-
	11 days	-17.56	-4.38	-3.03	-
12 days	-18.81	-4.41	-3.04	11.8	

332 Using data in **Table 6** and equation $Q = it$, where Q is the total amount of charge passed, i is applied
333 current density and t is time, it can be estimated that when anode is operated at 20 mA/m^2 current
334 density, it will perform satisfactorily up to approximately 15 years. The typical service life of
335 currently commercially available paint anode system is 15-20 years based on its physical detachment
336 from the surface without considering anode consumption. Hence, the service life of ZRP anode is
337 comparable. At the end of the test, the ZRP block was examined, as shown in **Fig.12**. It can be
338 observed that the whole ZRP block was covered with a white product. The powdered sample of the
339 white product was collected, dried and tested using XRD and XRF. XRF analysis showed that the
340 major component being zinc oxide (**Table 7**).

**Fig. 12-** White product observed on ZRP block at the end of anode life testing

341

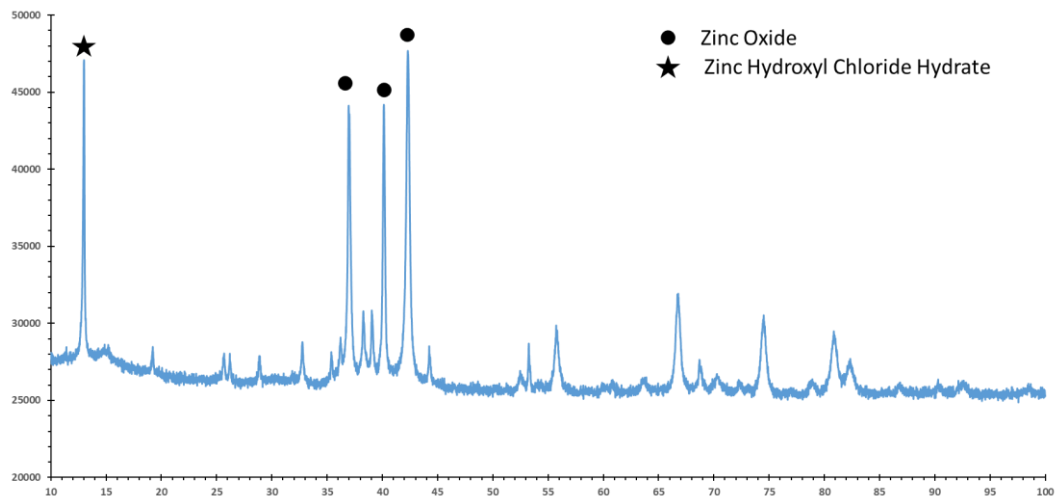
342

343

Table 7- XRF Analysis of white product

Main Component	Wt. %
ZnO	77
Na ₂ O	6
Cl	17

344 **Fig. 13** shows the X-ray diffractograms of the product. Zinc oxide and Zinc hydroxyl chloride hydrate
345 are identified from these specimens. Peaks corresponding to 42.3^o, 13.0^o of 2 Θ are identified, which
346 corresponds to zinc oxide and zinc hydroxyl chloride hydrate respectively. This confirms zinc in the
347 paint is oxidising to form zinc oxide/hydroxides during polarization. This might affect current and
348 potential distribution in the long run. Further, extensive durability testing is under study to determine
349 ZRP performance before this coating is considered as a viable product.

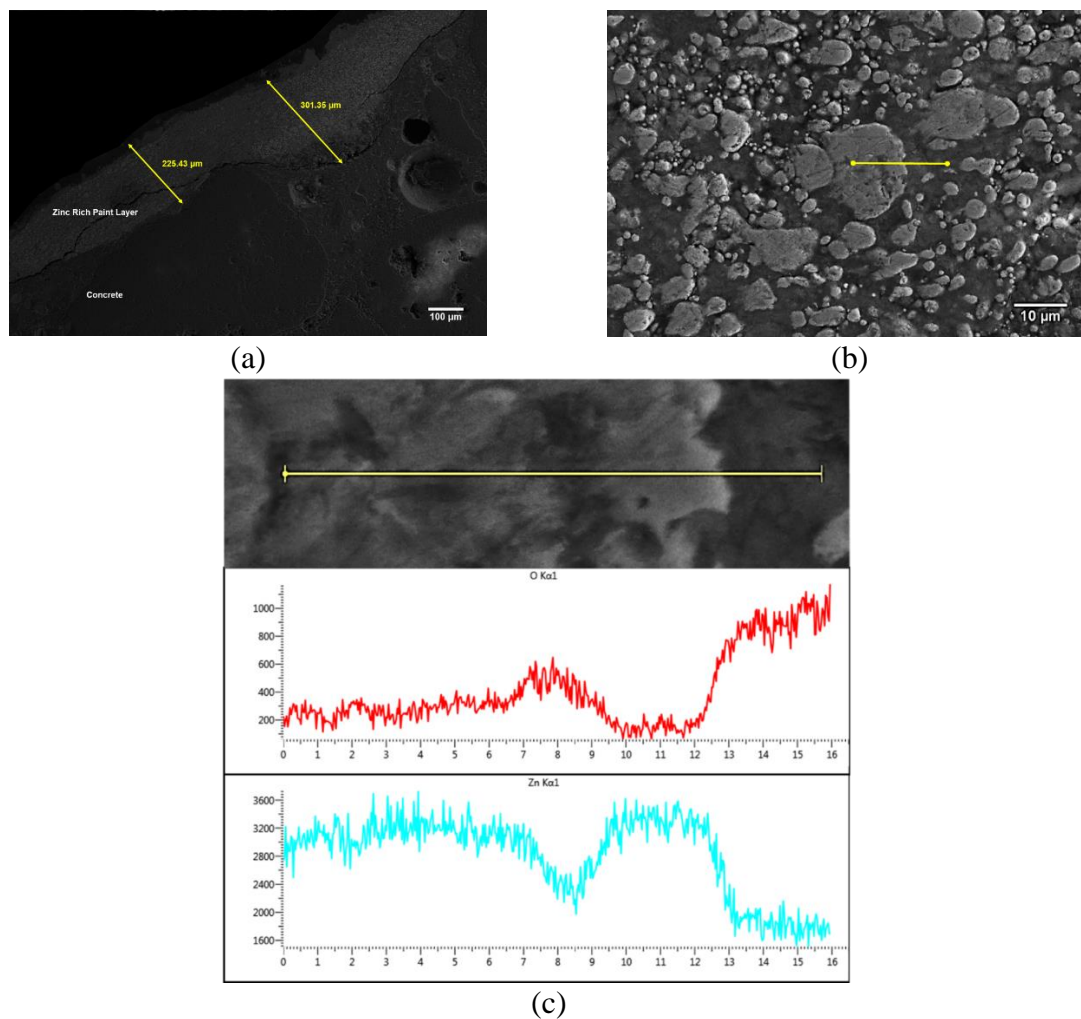


350 **Fig. 13-** XRD analysis of white product

351 **4.6 Microstructural Analysis**

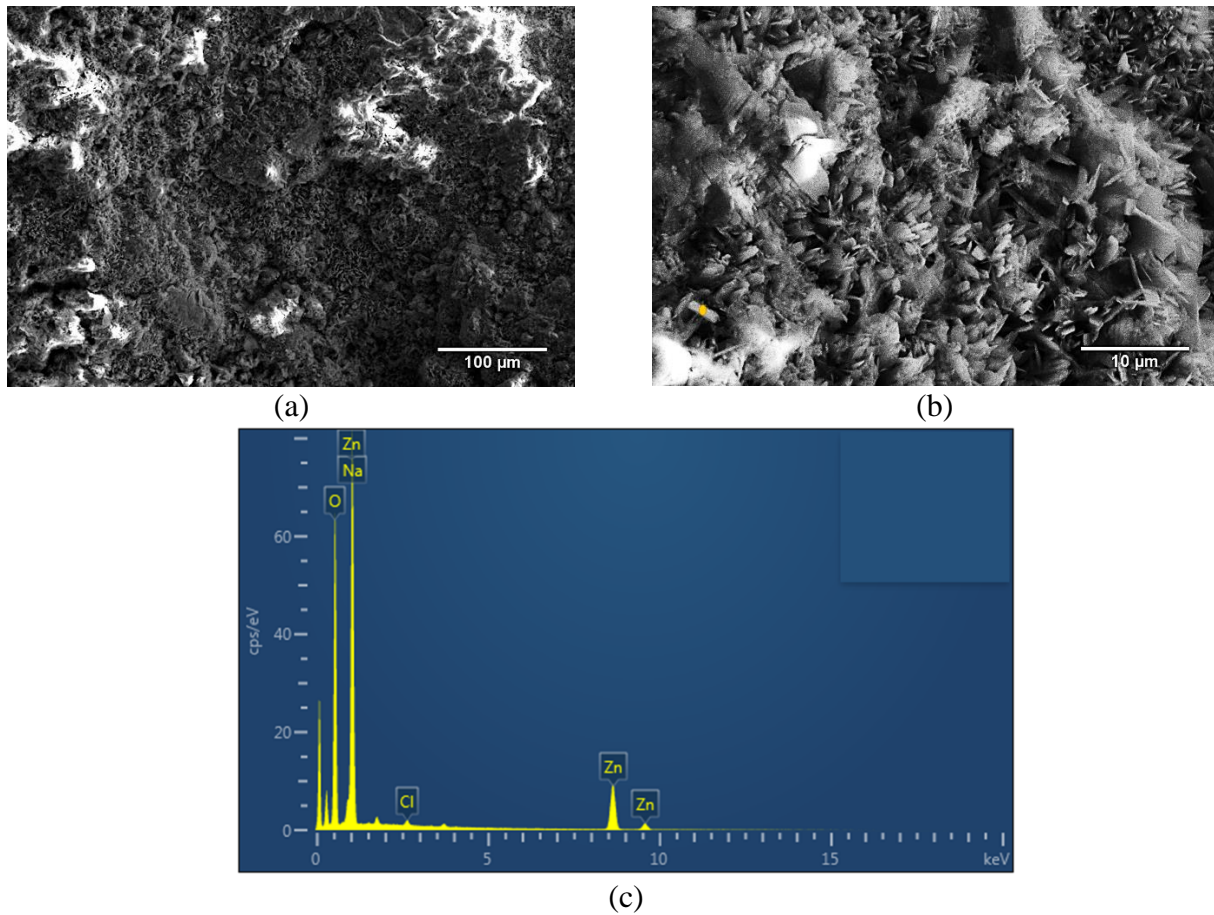
352 Coated concrete samples were collected after the polarization test on slabs and analysed using
353 SEM/EDS. **Fig.14(a)** shows SEM micrographs of ZRP-concrete interface after polarization,
354 depicting coating thickness between 200-350µm. **Fig.14(b)** shows a cross section of the coating
355 sample, in which zinc corrosion products on the surface of zinc particles were observed. A line scan
356 analysis was performed on one of the particles and results are shown in **Fig.14(c)**, which shows that
357 the zinc corrosion products were mainly composed of zinc and oxygen, suggesting the formation of
358 zinc oxide or zinc hydroxide. This could be due to the self-corrosion process of zinc particles (i.e.

359 zinc dissolution and oxygen reduction reaction occurred on the surface of zinc particles) at
360 zinc/electrolyte interface [58].



361 **Fig.14-** Cross- sectional analysis of ZRP concrete (a) cross-section of SEM micrograph (b) cross-
362 section of coating sample (c) line scan analysis

363
364 **Fig. 15** shows surface analysis of ZRP coated concrete samples from the coated side. Several small
365 hexagonal plates were observed, The EDS analysis of yellow marker in **Fig. 15(b)** is shown in **Fig.**
366 **15(c)**, depicting main peaks of zinc and oxygen, again suggesting the formation of ZnO. Similar
367 morphology was observed by Perkins and Bornholdt [59]. Surface charging by the electron beam was
368 observed to a varying degree, but generally was not a serious problem.



369 **Fig. 15-** SEM micrographs of surface analysis of coated sample at different magnifications (a) and
 370 (b). (c) shows corresponding EDS spectra of yellow marker in (b)

371 5.0 Summary and Conclusions

372 The research presented in this paper evaluates the feasibility of using ZRP as an anode of an ICCP
 373 system. Following conclusions can be drawn from the study:

- 374 • Results of electrochemical testing showed that ZRP conductive coating can be used successfully
 375 as an effective ICCP anode system and satisfy the performance criteria in accordance with BS EN
 376 ISO 12696 [37] standard.
- 377 • The ZRP coating showed satisfactory bond at the anode-concrete interface. The pull-off failure
 378 stress was 2.73 MPa satisfying the recommended required pull off strength according to BS EN
 379 1504-2:2004 [56].

- 380 • More uniform current distribution with the least potential drop across the ZRP coating anode was
381 obtained by using Anomet platinum clad wire primary anode when compared to MMO coated Ti
382 ribbon anode.
- 383 • Permeability results showed ZRP coating to be water vapour permeable, thus preventing long
384 term debondment and premature failure.
- 385 • Polarization results showed satisfactory performance of the ZRP anode with an optimum current
386 density of 12.5 mA/m² per anode surface area. The results satisfy 100 mV depolarization criterion
387 i.e. criterion (b) of BS EN 12696 [37].
- 388 • Anode was even capable of sustaining design current densities recommended in BS EN ISO
389 12696 at 1:1 steel: anode surface area ratio.
- 390 • The service life of anode was estimated from the accelerated service life test to be 15 years when
391 operated at 20 mA/m² current density.
- 392 • Microstructural analysis showed the formation of oxide/hydroxide products of zinc after
393 polarization. This might affect current and potential distribution in the long run.
- 394 • Further, extensive durability testing and comparison to other anodes such as carbon pigmented
395 paints are required to determine ZRP performance before this coating is considered as a viable
396 product and same is under study by authors.

397 **6.0 References**

- 398 [1] J. Román, R. Vera, M. Bagnara, A.M. Carvajal, W. Aperador, Effect of chloride ions on the corrosion of
399 galvanized steel embedded in concrete prepared with cements of different composition, *Int. J. Electrochem. Sci.*
400 9 (2014) 580–592.
- 401 [2] Popov, *Corrosion Engineering: Principles and Solved Problems*, 1st ed., Elsevier, Oxford, 2015.
402 doi:10.2307/23499350.
- 403 [3] Y. Lu, J. Hu, S. Li, W. Tang, Active and passive protection of steel reinforcement in concrete column using

- 404 carbon fibre reinforced polymer against corrosion, *Electrochim. Acta.* 278 (2018) 124–136.
405 doi:10.1016/j.electacta.2018.05.037.
- 406 [4] A. Goyal, H.S. Pouya, E. Ganjian, P. Claisse, A Review of Corrosion and Protection of Steel in Concrete, *Arab.*
407 *J. Sci. Eng.* 43 (2018). doi:10.1007/s13369-018-3303-2.
- 408 [5] D. Hong, W. Fan, D. Luo, V. Ge, Y. Zhu, Study and Application of Impressed Current Cathodic Protection
409 Technique for Atmospherically Exposed Salt- Contaminated Reinforced Concrete Structures, *ACI Mater. J.*
410 (1993) 3–7.
- 411 [6] R.B. Polder, W.H.A. Peelen, B.T.J. Stoop, E.A.C. Neeft, Early stage beneficial effects of cathodic protection in
412 concrete structures, *Mater. Corros.* 62 (2011) 105–110. doi:10.1002/maco.201005803.
- 413 [7] A. Goyal, H.S. Pouya, E. Ganjian, M. Tyrer, Concrete coating systems for corrosion prevention in reinforced
414 concrete structures, *Concr. Soc.* (2018) 22–24.
- 415 [8] A. Byrne, N. Holmes, B. Norton, State-of-the-art review of cathodic protection for reinforced concrete structures,
416 *Mag. Concr. Res.* 68 (2016) 1–14. doi:10.1680/jmacr.15.00083.
- 417 [9] J. Xu, W. Yao, Current distribution in reinforced concrete cathodic protection system with conductive mortar
418 overlay anode, *Constr. Build. Mater.* 23 (2009) 2220–2226. doi:10.1016/j.conbuildmat.2008.12.002.
- 419 [10] US Federal Highway Administration, Long-term effectiveness of cathodic protection systems on highway
420 structures, Publ. No. FHWA-RD-01-096, FHWA. (2001).
421 [http://scholar.google.com/scholar?hl=en&btnG=Search&q=intitle:Long-](http://scholar.google.com/scholar?hl=en&btnG=Search&q=intitle:Long-Term+Effectiveness+of+Cathodic+Protection+Systems+on+Highway+Structures#0)
422 [Term+Effectiveness+of+Cathodic+Protection+Systems+on+Highway+Structures#0](http://scholar.google.com/scholar?hl=en&btnG=Search&q=intitle:Long-Term+Effectiveness+of+Cathodic+Protection+Systems+on+Highway+Structures#0).
- 423 [11] H. Sun, L. Wei, M. Zhu, N. Han, J.H. Zhu, F. Xing, Corrosion behavior of carbon fiber reinforced polymer anode
424 in simulated impressed current cathodic protection system with 3% NaCl solution, *Constr. Build. Mater.* 112
425 (2016) 538–546. doi:10.1016/j.conbuildmat.2016.02.141.
- 426 [12] C. Christodoulou, G. Glass, J. Webb, S. Austin, C. Goodier, Assessing the long term benefits of Impressed Current
427 Cathodic Protection, *Corros. Sci.* 52 (2010) 2671–2679. doi:10.1016/j.corsci.2010.04.018.
- 428 [13] J.P. Broomfield, *Corrosion of Steel in Concrete: Understanding, Investigation and Repair*, Second Edition, 2nd
429 ed., Taylor and Francis, London and New York, 2006. doi:10.4324/9780203414606.
- 430 [14] R. Montoya, V. Nagel, J.C. Galv??n, J.M. Bastidas, Influence of irregularities in the electrolyte on the cathodic
431 protection of steel: A numerical and experimental study, *Mater. Corros.* 64 (2013) 1055–1065.

- 432 doi:10.1002/maco.201307040.
- 433 [15] A. Goyal, H.S. Pouya, E. Ganjian, A.O. Olubanwo, M. Khorami, Predicting the corrosion rate of steel in
434 cathodically protected concrete using potential shift, *Constr. Build. Mater.* 194 (2019).
435 doi:10.1016/j.conbuildmat.2018.10.153.
- 436 [16] B.S. Covino, G.R. Holcomb, S.J. Bullard, J.H. Russell, S.D. Cramer, J.E. Bennett, H.M. Laylor, Electrochemical
437 Aging of Humectant-Treated Thermal-Sprayed Zinc Anodes for Cathodic Protection, *Solutions.* (1999).
438 doi:10.1108/eb019364.
- 439 [17] B.S. Covino, S. Cramer, S. Bullard, G. Holcomb, J. Russel, Collins<WK, H. Laylor, C.B. Cryer, Performance of
440 zinc anodes for cathodic protection of reinforced concrete bridges, Albany Research Center, Albany, OR (US)
441 (2002).
- 442 [18] G.R. Holcomb, S.J. Bullard, B.S. Covino, S.D.C. Jr., C.B. Cryer, G.E. McGill, Electrochemical Aging of Thermal-
443 Sprayed Zinc Anodes on Concrete, *Proc. 9th Natl. Therm. Spray Conf. Therm. Spray Pract. Solut. Eng. Probl. pp*
444 (1996) 185–192.
- 445 [19] A.A. Sagiés, R.G. Powers, Sprayed-Zinc Sacrificial Anodes for Reinforced Concrete in Marine Service,
446 *Corrosion.* 52 (1996) 508–522.
- 447 [20] S.J. Bullard, S.D. Cramer, B.S. Covino Jr., G.R. Holcomb, G.E. McGill, Thermal-Sprayed Zinc Anodes for
448 Cathodic Protection of Steel-Reinforced Concrete Bridges, 2 (1996) 11.
- 449 [21] D.L. Leng, R.G. Powers, I.R. Lasa, Zinc Mesh Cathodic Protection Systems, *Corrosion.* (2000) Paper No.00031.
- 450 [22] G. Sergi, D. Whitmore, Performance of zinc sacrificial anodes for long-term control of reinforcement corrosion,
451 *NACE Int.* (2010) 1–17.
- 452 [23] H. Liao, D. Shah, Corrosion protection of reinforced concrete structures using embedded galvanic anodes,
453 *CORCON.* (2016).
- 454 [24] V.V.L.K. Rao, Experimental study on sacrificial cathodic protection of steel reinforcement in concrete beam,
455 *CORCON.* (2016).
- 456 [25] R. Brousseau, B. Arsenault, S. Dallaire, D. Rogers, T. Mumby, D. Dong, Sprayed Titanium Coatings for the
457 Cathodic Protection of Reinforced Concrete, 7 (1998) 193–196.
- 458 [26] S.D. Cramer, B.S. Covino, G.R. Holcomb, S.J. Bullard, W.K. Collins, R.D. Govier, R.D. Wilson, H.M. Laylor,

- 459 Thermal Sprayed Titanium Anode for Cathodic Protection of Reinforced Concrete Bridges, *J. Therm. Spray*
460 *Technol.* 8 (1999) 133–145. doi:10.1361/105996399770350665.
- 461 [27] K. Darowicki, J. Orlikowski, S. Cebulski, S. Krakowiak, Conducting coatings as anodes in cathodic protection,
462 *Prog. Org. Coatings.* 46 (2003) 191–196. doi:10.1016/S0300-9440(03)00003-1.
- 463 [28] J. Orlikowski, S. Cebulski, K. Darowicki, Electrochemical investigations of conductive coatings applied as
464 anodes in cathodic protection of reinforced concrete, *Cem. Concr. Compos.* 26 (2004) 721–728.
465 doi:10.1016/S0958-9465(03)00105-7.
- 466 [29] A.S.S. Sekar, V. Saraswathy, G.T. Parthiban, Cathodic Protection of Steel in Concrete Using Conductive Polymer
467 Overlays, *Int. J. Electrochem. Sci.* 2 (2007) 872–882.
- 468 [30] M. Poltavtseva, G. Ebell, J. Mietz, Electrochemical investigation of carbon-based conductive coatings for
469 application as anodes in ICCP system of reinforced concrete structures, *Mater. Corros.* (2015) 12696.
470 doi:10.1002/maco.201407680.
- 471 [31] M.-Á. Climent, J. Carmona, P. Garcés, Graphite–Cement Paste: A New Coating of Reinforced Concrete
472 Structural Elements for the Application of Electrochemical Anti-Corrosion Treatments, *Coatings.* 6 (2016) 32.
473 doi:10.3390/coatings6030032.
- 474 [32] L. Bertolini, F. Bolzoni, T. Pastore, P. Pedferri, Effectiveness of a conductive cementitious mortar anode for
475 cathodic protection of steel in concrete, *Cem. Concr. Res.* 34 (2004) 681–694.
476 doi:10.1016/j.cemconres.2003.10.018.
- 477 [33] S. Yehia, J. Host, Conductive concrete for cathodic protection of bridge decks, *ACI Mater. J.* 107 (2010) 577–
478 585.
- 479 [34] M.S. Anwar, B. Sujitha, R. Vedalakshmi, Light-weight cementitious conductive anode for impressed current
480 cathodic protection of steel reinforced concrete application, *Constr. Build. Mater.* 71 (2014) 167–180.
481 doi:10.1016/j.conbuildmat.2014.08.032.
- 482 [35] J. Carmona, P. Garcés, M.A. Climent, Efficiency of a conductive cement-based anodic system for the application
483 of cathodic protection, cathodic prevention and electrochemical chloride extraction to control corrosion in
484 reinforced concrete structures, *Corros. Sci.* (2015) 102–111. doi:10.1016/j.corsci.2015.04.012.
- 485 [36] M.M.S. Cheung, C. Cao, Application of cathodic protection for controlling macrocell corrosion in chloride
486 contaminated RC structures, *Constr. Build. Mater.* 45 (2013) 199–207. doi:10.1016/j.conbuildmat.2013.04.010.

- 487 [37] B.S. Institution, Cathodic protection of steel in concrete BS EN ISO 12696, Br. Stand. Inst. BS EN ISO (2016).
- 488 [38] J. Bennett, J.B. Bushman, J. Costa, P. Noyce, Field Application of Performance Enhancing Chemicals to
489 Metallized Zinc Anodes, Corrosion. paper no. (2000) Paper No.00031.
- 490 [39] G.T. Parthiban, T. Parthiban, R. Ravi, V. Saraswathy, N. Palaniswamy, V. Sivan, Cathodic protection of steel in
491 concrete using magnesium alloy anode, Corros. Sci. (2008). doi:10.1016/j.corsci.2008.08.040.
- 492 [40] J.P. Broomfield, Cathodic protection using thermal sprayed metals, in Concrete repair a practical guide. 1st edn.
493 ed. by Grantham, M., & Grantham, Mike. London and New York: Routledge, 2011.
- 494 [41] P. Chess, M., J. Broomfield, P., Cathodic Protection of Steel in Concrete and Masonry, 2nd ed., CRC Press, Boca
495 Raton, 2014.
- 496 [42] J.P. Broomfield, The Principles and Practice of Galvanic Cathodic Protection for Reinforced Concrete Structures-
497 Technical Notes 6, CPA Tech. NOTE. (2007).
- 498 [43] S.P. Holmes, G.D. Wilcox, P.J. Robins, G.K. Glass, A.C. Roberts, Responsive behaviour of galvanic anodes in
499 concrete and the basis for its utilisation, Corros. Sci. 53 (2011) 3450–3454. doi:10.1016/j.corsci.2011.06.026.
- 500 [44] S.J. Bullard, S. Cramer, Final Report Effectiveness of Cathodic Protection SPR 345 Sophie J . Bullard , Stephen
501 Cramer (retired), Bernard Covino National Energy Technology Laboratory 1450 Queen Ave . SW, (2009).
- 502 [45] M.J. Dugarte, A.A.Sagues, Sacrificial Point Anodes for Cathodic Prevention of Reinforcing Steel in Concrete
503 Repairs : Part 1 — Polarization Behavior, Corrosion. 70 (2014) 303–317.
- 504 [46] R. Brousseau, M. Arnott, B. Baldock, Laboratory performance of zinc anodes for impressed current cathodic
505 protection of reinforced concrete, Corrosion. 51 (1995) 639–644. doi:10.5006/1.3293625.
- 506 [47] H. Marchebois, C. Savall, J. Bernard, S. Touzain, Electrochemical behavior of zinc-rich powder coatings in
507 artificial sea water, Electrochim. Acta. 49 (2004) 2945–2954. doi:10.1016/j.electacta.2004.01.053.
- 508 [48] C.M. Abreu, M. Izquierdo, M. Keddam, X.R. Nóvoa, H. Takenouti, Electrochemical behaviour of zinc-rich epoxy
509 paints in 3% NaCl solution, Electrochim. Acta. 41 (1996) 2405–2415. doi:10.1016/0013-4686(96)00021-7.
- 510 [49] British Standards, BS 1881 Part 125 : Methods for mixing and sampling fresh concrete in the laboratory, (2013)
511 1–8. doi:Construction Standard, CS1:2010.
- 512 [50] N. International, TM 0294-2007 Test Method Testing of Embeddable Impressed Current Anodes for Use in
513 Cathodic Protection of Atmospherically Exposed Steel-Reinforced Concrete, (2007).

- 514 [51] A. Goyal, E. Ganjian, H.S. Pouya, Bond Strength Behaviour of Zinc Rich Paint Coating on Concrete Surface, in:
515 Young Res. Forum IV Innov. Constr. Mater., Newcastle, 2018: pp. 21–25.
- 516 [52] ASTM International, ASTM D7234-12 Standard Test Method for Pull-Off Adhesion Strength of Coatings on
517 Concrete Using Portable Pull-Off Adhesion Testers, ASM Int. (2012) 1–9. doi:10.1520/D7234-12.2.
- 518 [53] British Standards Institution BSI, BS EN 1062-3:2008: Paints and varnishes - Coating materials and coating
519 systems for exterior masonry and concrete Part 3: Determination of liquid water permeability, BSI. 3 (2008).
- 520 [54] British Standards Institution, BS EN ISO 7783 : 2018: Paints and varnishes - Determination of water- vapour
521 transmission properties - Cup method, Br. Stand. Inst. (2018).
- 522 [55] J.G. Legoux, S. Dallaire, Adhesion mechanisms of arc-sprayed zinc on concrete, J. Therm. Spray Technol. 4
523 (1995) 395–400. doi:10.1007/BF02648641.
- 524 [56] British Standards Institution, Products and systems for the protection and repair of concrete structures -
525 Definitions, requirements, quality control and evaluation of conformity. Part 2: Surface protection systems for
526 concrete, Br. Stand. Inst. 1504–2 (2004). doi:10.1017/CBO9781107415324.004.
- 527 [57] P. Chess, Gronvold, Karnov, Cathodic protection of steel in concrete, 1st edn. ed. London: E &F Spon, 37-59.
528 1998.
- 529 [58] Y. Cubides, S.S. Su, H. Castaneda, Influence of zinc content and chloride concentration on the corrosion
530 protection performance of zinc-rich epoxy coatings containing carbon nanotubes on carbon steel in simulated
531 concrete pore environments, Corrosion. 72 (2016) 1397–1423. doi:10.5006/2104.
- 532 [59] J. Perkins, R.A. Bornholdt, The corrosion product morphology found on sacrificial zinc anodes, Corros. Sci. 17
533 (1977) 377–384. doi:10.1016/0010-938X(77)90027-0.

534 **Declaration of Interest**

535 We wish to confirm that there are no known conflicts of interest associated with this publication and
536 there has been no significant financial support for this work that could have influenced its outcome.